

On Flavourful Easter eggs for New Physics hunger and Lepton Flavour Universality violation

Marco Ciuchini^a, António M. Coutinho^a, Marco Fedele^{b,c}, Enrico Franco^c, Ayan Paul^c, Luca Silvestrini^c and Mauro Valli^c

^a*INFN, Sezione di Roma Tre, Via della Vasca Navale 84, I-00146 Roma, Italy*

^b*Dipartimento di Fisica, Università di Roma “La Sapienza”, P.le A. Moro 2, I-00185 Roma, Italy*

^c*INFN, Sezione di Roma, P.le A. Moro 2, I-00185 Roma, Italy*

E-mail: marco.fedele@uniroma1.it, ayan.paul@roma1.infn.it,
mauro.valli@roma1.infn.it

ABSTRACT: In the world of media, Easter eggs are commonly associated to the internal jokes and/or secret messages usually hidden e.g. in computer gaming and hi-tech software. In this work, we take advantage of this terminology to motivate the search for New Physics Beyond the Standard Model of Particle Physics in the radiative and (semi-)leptonic channels of rare B meson decays. Within the standard approach of effective field theory of weak interactions for $\Delta B = 1$ transitions, we look for possibly unexpected subtle NP effects, aka “flavourful Easter eggs”. We perform a Bayesian analysis that takes into account the state-of-the-art of the experimental information concerning these processes, including the suggestive measurements from LHCb of R_K and R_{K^*} , the latter available only very recently. We parametrize NP contributions to $b \rightarrow s$ transitions in terms of shifts of Wilson coefficients of the electromagnetic dipole and semileptonic operators, assuming CP-conserving effects, but allowing in general for violation of lepton flavour universality. We show how the optimistic/conservative hadronic estimates can impact quantitatively the size of NP extracted from the fit.

Contents

1	Introduction	1
2	Theoretical framework of the analysis	3
2.1	New Physics benchmarks for $\Delta B = 1$	4
2.2	Treatment of the Hadronic Uncertainties	5
3	Bayesian fit of the dipole and semileptonic operators	7
3.1	Experimental information considered	7
3.2	Results of the global fit	8
4	Discussion	11
A	Tables	15

1 Introduction

More than sixty years ago, the roots of what we know today as the Standard Model (SM) of Particle Physics progressed to the birth of Flavour Physics [1]. In the decades that have followed, the flavour structure of the SM has been experimentally tested and well established. The tremendous progress of the experimental facilities has probed the flavour of the SM to an exquisite level of precision [2], along with the substantial effort on the part of the theoretical community to go well beyond leading order computations [3]. From this perspective of “precision tests”, radiative and (semi-)leptonic $\Delta B = 1$ processes, related at the partonic level to $b \rightarrow s\gamma, s\ell\ell$ transitions, occupy a special place in probing the SM theoretical content and its possible extensions in terms of New Physics (NP) models [4, 5].

Firstly, these rare B meson decays belong to the class of flavour-changing neutral current (FCNC) processes, that are well known to be sensitive probes of Beyond the Physics Standard Model (BSM): In fact – within the SM – the flavour structure of the theory allows FCNC to arise only at loop level and consequently the latter are suppressed by the GIM mechanism [6]. This allows for significant room for heavy new degrees of freedom to sizably contribute to these rare processes.

Secondly, from the experimental side, the study of rare B meson decays offers us some of the most precise measurements amongst the $|\Delta F| = 1$ processes. For instance, the measurement of the inclusive branching fraction of $B \rightarrow X_s\gamma$ is currently performed with an experimental sensitivity better than one part per ten thousand [7–9], while the study of an exclusive mode such as $B \rightarrow K^*\ell\ell$ allows a detailed analysis of the angular distribution of the four final states of the decay, yielding rich experimental information in terms of angular functions of the dilepton invariant mass, with full kinematic coverage of the latter

[10] and – starting from Ref. [11] – also with available experimental correlations among the several angular observables.

In B Physics, the recent years have been characterized by the emergence of a striking pattern of anomalies in multiple independent studies of some of these rare $b \rightarrow s$ transitions [12]. Of particular importance, the measurement of the P'_5 angular observable [13–16] stands out from all the other ones related to the angular distribution of $B \rightarrow K^* \mu \mu$; first realized by the LHCb collaboration [17, 18] and later on also by the Belle collaboration [19], the experimental analysis of P'_5 in the large recoil region of the decay points to a deviation of about 3σ with respect to the SM prediction presented in Ref. [20]. The latter, however, suffers from possible hadronic uncertainties which are sometimes even hard to guesstimate [21–24], and this observation has been at the origin of a quite vivid debate in the recent literature about the size of (possibly) known and (yet) unknown QCD power corrections to the amplitude of this process in the infinite mass limit [25–28]. To corroborate even more the cumbersome picture of the “ P'_5 anomaly”, two new independent measurements of this angular observable (among others) have been recently released by ATLAS [29] and CMS [30] collaborations, showing respectively an appreciable increase and reduction of the tension between data and the SM prediction in the same reference, as reported by these experiments.

For the sake of completeness, one should also remark that other smaller tensions have been around meanwhile, concerning the measurement of differential branching fractions of $B \rightarrow K \mu \mu$ [31] and $B_s \rightarrow \phi \mu \mu$ [32]. It is worth noting that, while for the latter mode an explanation in terms of hadronic physics may be easily conceivable, the theoretical computation of the former seems to be under control [33]. Moreover, a recent LHCb analysis in the full kinematic region of the differential branching fraction of the $K^+ \mu^+ \mu^-$ channel – aiming at disentangle the short distance part of the amplitude from the long distance contribution at the charm resonance – indicates towards a discrepancy from the “SM only” scenario [34].

Quite surprisingly, a possible smoking gun for NP in rare B meson decays already came out in 2014, when the LHCb collaboration presented for the first time the measurement of the ratio of branching fractions [35]:

$$R_{K_{[1.1,6]}} \equiv \frac{Br(B^+ \rightarrow K^+ \mu^+ \mu^-)}{Br(B^+ \rightarrow K^+ e^+ e^-)} = 0.745^{+0.090}_{-0.074} \pm 0.036, \quad (1.1)$$

where the subscript refers to the dilepton mass range going from 1.1 to 6 GeV^2 . This experimental value shows, within errors, a deviation of about 2.6σ with respect to the standard theoretical prediction. Indeed, the SM value of R_K in the bin provided by the LHCb collaboration is expected to deviate from unity only at the percent level [36]. In fact, contrary to observables such as P'_5 , it is important to stress that R_K may be, in general, regarded as insensitive to QCD effects. From the model building point of view, R_K can be certainly considered as quite informative, hinting at a UV completion of the SM where Lepton Flavour Universality violation (LFUV) takes place in the flavour-violating couplings of new heavy degrees of freedom, e.g. leptoquarks and/or Z' gauge bosons [37–57]. Most importantly, the tantalizing correlation of this signature of LFUV with the P'_5 anomaly, suggested by

several global analyzes [4, 58–62] has triggered different proposals of measurements of such effect in the angular analysis of the $K^*\ell\ell$ channel [63, 64]. Interestingly enough, an analysis from the Belle collaboration aiming to separate the leptonic flavours in $B \rightarrow K^*\ell\ell$ [65], shows a consistent $\sim 2.6 \sigma$ deviation from the SM prediction reported in Ref. [20] in the dimuon leptonic final state only. This is compatible with previous experimental findings related only to the mode with muonic final state.

Sitting on similar theoretical grounds as R_K , another intriguing ratio of the B decay branching fractions can be measured in the K^* channel:

$$R_{K^*}^{[0.045, 1.1]} \equiv \frac{Br(B^+ \rightarrow K^{*+}\mu^+\mu^-)}{Br(B^+ \rightarrow K^{*+}e^+e^-)} = 0.660_{-0.070}^{+0.110} \pm 0.024, \quad (1.2)$$

$$R_{K^*}^{[1.1, 6]} = 0.685_{-0.069}^{+0.113} \pm 0.047. \quad (1.3)$$

These measurements for the low- q^2 bin and the central- q^2 one have just been presented to the community by the LHCb collaboration [66], pointing again to a discrepancy of about 2σ with respect to the expected SM prediction – again equal to 1 up to QED corrections of a few percent [36] – and yielding more than a 3σ deviation when naively combined with the measurement of R_K . Note that with higher degree of braveness (or, depending on the taste of the reader, of unconsciousness), the disagreement of the SM with precision B physics may reach the exciting level of $\gtrsim 5 \sigma$ level when one naively combines together the single significances coming from R_{K,K^*} ratios, P'_5 measurements and the minor deviations observed in the other exclusive branching fractions.

Given the excitement of these days for all the above hints on a possible NP discovery in B rare meson decays, in this work we make our first steps towards a positive attitude in the search of a definite BSM pattern aimed at addressing these compelling B anomalies. We perform our study in a model-independent fashion, within the framework of effective field theories for weak interactions [67, 68]. In particular, in Section 2 we define the setup characterizing the whole global analysis, presenting five different benchmark scenarios for NP, together with a discussion about two different approaches in the estimate of the hadronic uncertainties that can affect quantitatively our final results. In Section 3, we list all the experimental measurements we use to construct the likelihood in our fit, and we discuss in detail our most important findings. The latter are effectively depicted in Figs. 1–6, and collected in Tables 2–5 in Appendix A. In Section 4 we summarize our conclusions, with the attempt of suggesting the next steps needed to draw a more precise picture of the possible NP lying behind this set of exciting B decay anomalies.

2 Theoretical framework of the analysis

In this Section we present the effective field theory framework at the basis of this work and introduce the benchmark scenarios we have decided to focus on for our study of NP effects in rare B decays. We then illustrate the two distinct broad classes of assumptions that characterize our global analysis: The case where we take an optimistic attitude towards the estimate of hadronic uncertainty plaguing the amplitude of both $B \rightarrow K^*$ and $B_s \rightarrow \phi$

channels, and a more refined one where we aim at providing a more conservative approach. All the results in Section 3.2 will be classified under these two different setups.

2.1 New Physics benchmarks for $\Delta B = 1$

Integrating out the heavy degrees of freedom, the resulting effective Hamiltonian of weak interactions for $b \rightarrow s\gamma, (s)\ell\ell$ transitions involves the following set of dimension six operators within the SM [69]:

$$\begin{aligned}
Q_1^p &= (\bar{s}_L \gamma_\mu T^a p_L)(\bar{p}_L \gamma^\mu T^a b_L), \\
Q_2^p &= (\bar{s}_L \gamma_\mu p_L)(\bar{p}_L \gamma^\mu b_L), \\
P_3 &= (\bar{s}_L \gamma_\mu b_L) \sum_q (\bar{q} \gamma^\mu q), \\
P_4 &= (\bar{s}_L \gamma_\mu T^a b_L) \sum_q (\bar{q} \gamma^\mu T^a q), \\
P_5 &= (\bar{s}_L \gamma_{\mu 1} \gamma_{\mu 2} \gamma_{\mu 3} b_L) \sum_q (\bar{q} \gamma^{\mu 1} \gamma^{\mu 2} \gamma^{\mu 3} q), \\
P_6 &= (\bar{s}_L \gamma_{\mu 1} \gamma_{\mu 2} \gamma_{\mu 3} T^a b_L) \sum_q (\bar{q} \gamma^{\mu 1} \gamma^{\mu 2} \gamma^{\mu 3} T^a q), \\
Q_{8g} &= \frac{g_s}{16\pi^2} m_b \bar{s}_L \sigma_{\mu\nu} G^{\mu\nu} b_R, \\
Q_{7\gamma} &= \frac{e}{16\pi^2} m_b \bar{s}_L \sigma_{\mu\nu} F^{\mu\nu} b_R, \\
Q_{9V} &= \frac{\alpha_e}{4\pi} (\bar{s}_L \gamma_\mu b_L)(\bar{\ell} \gamma^\mu \ell), \\
Q_{10A} &= \frac{\alpha_e}{4\pi} (\bar{s}_L \gamma_\mu b_L)(\bar{\ell} \gamma^\mu \gamma^5 \ell),
\end{aligned} \tag{2.1}$$

where $\ell = e, \mu$ and we have neglected the chirally suppressed SM dipoles. The $\Delta B = 1$ effective Hamiltonian can be casted in full generality as a combination of two distinct parts:

$$\mathcal{H}_{\text{eff}}^{\Delta B=1} = \mathcal{H}_{\text{eff}}^{\text{had}} + \mathcal{H}_{\text{eff}}^{\text{sl}+\gamma}, \tag{2.2}$$

where, within the SM, the hadronic term involves the first seven operators in Eq. (2.1):

$$\mathcal{H}_{\text{eff}}^{\text{had}} = \frac{4G_F}{\sqrt{2}} \left[\sum_{p=u,c} \lambda_p \left(C_1 Q_1^p + C_2 Q_2^p \right) - \lambda_t \left(\sum_{i=3}^6 C_i P_i + C_8 Q_{8g} \right) \right], \tag{2.3}$$

while the second piece includes the electromagnetic dipole and semileptonic operators:

$$\mathcal{H}_{\text{eff}}^{\text{sl}+\gamma} = -\frac{4G_F}{\sqrt{2}} \lambda_t \left(C_7 Q_{7\gamma} + C_9 Q_{9V} + C_{10} Q_{10A} \right), \tag{2.4}$$

with λ_i corresponding to the CKM combination $V_{ib} V_{is}^*$ for $i = u, c, t$ and where $C_{i=1,\dots,10}$ are the Wilson coefficients (WCs) encoding the short-distance physics of the theory. All the SM WCs of this work are evolved from the mass scale of the W boson down to $\mu_b = 4.8$ GeV, using the state-of-the-art of perturbative QCD and QED calculations for the matching conditions [70–72] and the anomalous dimension matrix elements [72–75] relevant for the processes considered in this analysis.

While a general UV completion of the SM may enter in the effective couplings present in both the pieces of Eq. (2.2), general NP effects in $b \rightarrow s\gamma, (s)\ell\ell$ can be phenomenologically

parametrized as shifts of the Wilson coefficients of the electromagnetic and semileptonic operators at the typical scale of the processes, μ_b . In particular, the most general basis for NP effects in radiative and (semi-)leptonic B decays can be enlarged by the presence of scalar, pseudo-scalar and tensorial semileptonic operators, together with right-handed quark currents as the analogue of $Q_{7\gamma}, Q_{9V}, Q_{10A}$ SM operators [21, 76]. In this work, motivated by previous interesting findings concerning LFUV [59–61] and the measurement of R_K and R_{K^*} , we focus on the contributions of NP appearing as shifts of the SM WCs related to the electromagnetic dipole and semileptonic operators with left-handed quark currents only. A comprehensive analysis with different chiral structures as well as a more general effective theory framework will be presented elsewhere [77]. Furthermore, we restrict ourselves to CP-conserving effects, taking NP WCs to be real. For NP in semileptonic operators we discriminate between couplings to muon and electron fields both in the axial and vector leptonic currents. We characterize our phenomenological analysis for NP through five different benchmark scenarios, studying the impact of combinations of the following NP WCs :

- (I) $C_{9,\mu,e}^{NP}$ varied in the range $[-4, 4]$, i.e. adding to the SM two NP parameters;
- (II) $C_{9,\mu}^{NP}, C_{10,\mu}^{NP}$ varied in the range $[-4, 4]$, adding to the SM again two NP parameters;
- (III) C_7^{NP} varied in the range $[-0.5, 0.5] + \text{(I)}$, i.e. a scenario with three NP parameters;
- (IV) similar to latter case, but with C_{10}^{NP} in place of C_9^{NP} , i.e. adding again to the SM three NP parameters;
- (V) similar to the third case, but implementing the correlation $C_{10,\mu,e}^{NP} = -C_{9,\mu,e}^{NP}$, i.e. a set of NP scenarios again described by three different parameters.

We remark that while benchmarks (I) and (II) have been already studied in literature, none of the other cases has been analyzed so far. In particular, NP scenarios (III) and (IV) allow us to study, for the first time, the interesting impact of a NP radiative dipole operator in combination with vector-like and axial-like LFUV effects generated by NP. Most interestingly, scenario (V) allows us to explore the correlation $C_9^{NP} = -C_{10}^{NP}$, possibly hinting at a $SU(2)_L$ preserving BSM theory. As an additional interesting case to explore, we eventually aim to generalize the study of case (V), considering the broader correlation $C_9^{NP} = g_{VA} C_{10}^{NP}$, varying g_{VA} in the range $[-2, 2]$.

We wish to stress that all of the five benchmarks defined above will be studied for the first time under two different approaches in the estimate of QCD hadronic power corrections, as presented in Section 2.2.

2.2 Treatment of the Hadronic Uncertainties

In our previous papers [24, 27], we went into considerable detail on the treatment of hadronic contributions in the angular analysis of $B \rightarrow K^* \ell \ell$. Our approach there was to study how large these contributions can be assuming that the LHCb data on branching fractions and angular distributions of these decay modes could be described within the SM. For

that purpose we considered four scenarios for the hadronic contributions, with increasing theoretical input from the phenomenological analysis presented in Ref. [78]. The underlying functional form that we used for the hadronic contribution was given by:

$$\begin{aligned} h_\lambda(q^2) &= \frac{\epsilon_\mu^*(\lambda)}{m_B^2} \int d^4x e^{iqx} \langle \bar{K}^* | T \{ j_{\text{em}}^\mu(x) \mathcal{H}_{\text{eff}}^{\text{had}}(0) \} | \bar{B} \rangle \\ &= h_\lambda^{(0)} + \frac{q^2}{1 \text{ GeV}^2} h_\lambda^{(1)} + \frac{q^4}{1 \text{ GeV}^4} h_\lambda^{(2)}, \end{aligned} \quad (2.5)$$

where we fitted for the complex, helicity dependent, coefficients h_λ^i , ($i = 0, 1, 2$) and ($\lambda = 0, +, -$) using the data and the phenomenological model in [78].

In this work we proceed to study the possible existence of NP contributions in semileptonic and radiative $b \rightarrow s$ decays which requires a re-evaluation of the hadronic uncertainties. We also need to address modes that were not considered in our previous works, namely $B \rightarrow K\ell\ell$, $B \rightarrow \phi\ell\ell$ and $B \rightarrow \phi\gamma$. For the sake of simplicity, to address hadronic contributions we use the same functional parameterization as given in Eq. (2.5). However, we limit ourselves to only two hadronic models. The first, corresponding to the most widely used assumption, relies completely on the phenomenological model in [78] below $q^2 < 4m_c^2$. The second is a more conservative approach, where we impose the latter only in the large recoil region at $q^2 \leq 1$ while letting the data drive the hadronic contributions in the higher invariant mass region. We will refer to the first approach as phenomenological model driven (PMD) and the second as phenomenological model and data driven (PDD). In our fit we vary the h_λ^i parameters over generous ranges that are constrained by the phenomenological model and measurements at varying degrees in the two approaches. More detailed discussion on these can be found in [24, 27].

In contrast to $B \rightarrow K^*\ell\ell$, the decay $B \rightarrow K\ell\ell$ has been studied in greater detail in [33], where the authors show that the hadronic uncertainties are relatively smaller than the former case. These QCD power corrections can be broadly classified into hard gluon and soft gluon contributions. The former is difficult to calculate in the LCSR approach, as explained in the cited work, and hence the authors use the QCD factorization (QCDF) approach to estimate these as done in Ref. [79]. The soft gluon contributions are calculated using the same procedure as in Ref. [78]. A comparison of the LCSR estimate of the soft gluon contribution and the QCDF estimate of the hard gluon contribution reveals that the two are almost comparable in magnitude. In our computation we use the QCDF formalism from Ref. [79] since the explicit analytic formulae are available. We do not use the numerical results of Ref. [33].

The long distance contributions for $B_s \rightarrow \phi\ell\ell$ and $B_s \rightarrow \phi\gamma$ follow a similar theoretical derivation as those for $B \rightarrow K^*\ell\ell$ and $B \rightarrow K^*\gamma$, respectively, barring the fact that the spectator quark in the former is different from that in the latter. No theoretical calculations are available for the $B_s \rightarrow \phi$ decays and one has to rely on the estimates done for the $B \rightarrow K^*$ decays to get a handle on the long distance contributions. The spectator quark effects can come through the hard spectator scattering involving matrix elements of Q_2 , P_6 and Q_{8g} computable in QCD factorization [79] which we include in our computation. However, we do not include the sub-leading, and numerically small, QCDF power corrections to

spectator scattering involving Q_{8g} [80–82] and contributions to weak spectator scattering involving Q_{8g} beyond QCDF that have been computed in LCSR [83–85].

The effect of the difference in these spectator contributions is expected to be low firstly because they are numerically small and, secondly, because the effect is proportional to the small flavour $SU(3)$ breaking. Different approaches in relating the long distance contributions in the $B \rightarrow K^*$ channels to the ones in the $B \rightarrow \phi$ channels have been used in the literature [59, 60, 86], which vary in the degree of correlation between the two. While Ref [60] uses uncorrelated hadronic uncertainties, Refs. [59, 86] have left the two contributions highly correlated noting that the spectator contribution is expected to be numerically small. We take an approach similar to the latter considering the insensitivity of the current data to such small effects and assume the hadronic uncertainties are fully correlated, even though it is a very optimistic attitude. We leave a more detailed analysis of this assumption by relaxing the correlation between the hadronic contributions in the two modes to a future work.

3 Bayesian fit of the dipole and semileptonic operators

3.1 Experimental information considered

In this section we discuss the experimental measurements we use in the likelihood of our fit. Please note that for the exclusive modes we make use of measurements in the large recoil region only. Our choice harbours on the fact that the QCD long distance effects in the low recoil region are substantially different from the large recoil regime [87–90] and would require a dedicated analysis. For the fit in this study we consider the following experimental information:

- $B \rightarrow K^* \ell \ell$

For the $B \rightarrow K^* \mu \mu$ channel we use the LHCb measurements of CP-averaged angular observables extracted by means of the unbinned maximum likelihood fit, along with the provided correlation matrix [18]. Moreover, we employ the recent results for CP-averaged angular observables from ATLAS [29] and the ones measured by CMS [30, 91]¹ as well. Finally, we use the CP-averaged optimized angular observables recently measured by Belle [65]². Regarding the differential branching fractions, we use the recently updated measurements from LHCb [92] and the ones from CMS [91]. For the $B \rightarrow K^* e e$ channel we consider the LHCb results from [93] and the Belle results from [65]. R_{K^*} is taken from the value recently presented by LHCb [66].

Our theoretical predictions are computed in the helicity basis, whose relevant expressions can be found in [21]; the same framework is employed to study $B \rightarrow K^* \gamma$,

¹For all CMS data we use the 7, 8 TeV combined results, which can be found in <https://twiki.cern.ch/twiki/bin/view/CMSPublic/PhysicsResultsBPH13010>.

²Belle measures the $B^0 \rightarrow K^{*0} \mu \mu$ channel and the $B^+ \rightarrow K^{*+} \mu \mu$ one all together, without providing the mixture. On the theoretical side, we can therefore use these measurements under the approximation that QCD power corrections differentiating the amplitudes of the two channels are small. We have numerically checked that the impact of known QCD power corrections [79] is indeed at the percent level in the observables of interest.

$B_s \rightarrow \phi\mu\mu$, $B_s \rightarrow \phi\gamma$ and $B \rightarrow K\ell\ell$ channels. For the latter, we use the full set of form factors extrapolated from the lattice results, along with the provided correlation matrix [94]; for the remaining channels, we use the full set of form factors estimated combining LCSR and lattice results, along with the correlation matrices [95]. For the remaining factorizable and non-factorizable QCD power corrections, we refer to Sec. 2.2.

- $B \rightarrow K^*\gamma$

We include in our analysis the HFAG average for the branching fractions from [2].

- $B_s \rightarrow \phi\mu\mu$

We consider the LHCb CP-averaged angular observables and differential branching fractions measurements, along with the provided correlation matrix [32].

- $B_s \rightarrow \phi\gamma$

We use the LHCb measurement of the branching fraction from [96].

- $B \rightarrow K\ell\ell$

We employ the LHCb measurement of $B \rightarrow Kee$ differential branching fraction and R_K from [35]. We also include in our analysis the previous LHCb measurement of $B \rightarrow K\mu\mu$ branching fraction, available also at large recoil from [31].

- $B \rightarrow X_s\gamma$

We use the HFAG average from [2]. We perform our theoretical computation at NNLO in α_s and NLO in α_{em} , following [97] and references therein.

- $B_s \rightarrow \mu\mu$

We consider the latest measurement from LHCb [98] and do not consider the measurement from CMS [99], which has the same central value of LHCb, but larger uncertainty. Moreover, we chose not to use results for $B_d \rightarrow \mu\mu$, since there are only upper bounds for this decay channel so far [98, 99]. Our theoretical predictions include NLO EW corrections, as well as NNLO QCD correction, following the detailed expression in [100].

3.2 Results of the global fit

In this section we present the main results of our work. We perform this study using the `HEPfit` code [101] relying on its Markov Chain Monte Carlo based Bayesian analysis implemented with `BAT` [102]. We fit to the data using 18 free parameters that characterize the non-factorizable power corrections as was done in [24]. We assign to the hadronic parameters and the NP WCs flatly distributed priors in the relevant ranges mentioned in Section 2. The remaining parameters used in the fit are listed in Table 1. To better analyze the different scenarios, we introduce the Information Criterion [103, 104], defined as

$$IC = -2\overline{\log L} + 4\sigma_{\log L}^2, \quad (3.1)$$

where $\overline{\log L}$ is the average of the log-likelihood and $\sigma_{\log L}^2$ is its variance. Preferred models are expected to give smaller IC values. This measure takes into account the variation in the

Parameters	Mean Value	Uncertainty	Reference
$\alpha_s(M_Z)$	0.1185	0.0005	[105]
μ_W (GeV)	80.385	—	
m_t (GeV)	173.34	0.76	[106]
$m_c(m_c)$ (GeV)	1.28	0.02	[107]
$m_b(m_b)$ (GeV)	4.17	0.05	[108]
f_{B_s} (MeV)	226	5	[109]
f_{B_s}/f_{B_d}	1.204	0.016	[109]
$\Delta\Gamma_s/\Gamma_s$	0.129	0.009	[2]
λ	0.2250	0.0006	[110, 111]
A	0.829	0.012	[110, 111]
$\bar{\rho}$	0.132	0.018	[110, 111]
$\bar{\eta}$	0.348	0.012	[110, 111]
$f_{K^*, }$ (MeV)	204	7	[95]
$f_{K^*,\perp}(1\text{GeV})$ (MeV)	159	6	[95]
$f_{\phi, }$ (MeV)	233	4	[95]
$f_{\phi,\perp}(1\text{GeV})$ (MeV)	191	4	[95]
λ_B (MeV)	350	150	[112]
$a_1(\bar{K}^*)_{\perp, }$	0.2	0.1	[79, 113]
$a_2(\bar{K}^*)_{\perp, }$	0.05	0.1	[79, 113]
$a_2(\phi)_{\perp, }$	0.23	0.08	[95]
$a_1(K)_{\perp, }$	0.17	—	[114]
$a_2(K)_{\perp, }$	0.115	—	[114]

Table 1. *Parameters used in the analysis. The Gegenbauer parameters and λ_B have flat priors with half width reported in the third column. The remaining ones have Gaussian priors. Meson masses, lepton masses, s -quark mass and electroweak couplings are fixed at the PDG value [105].*

inference on the goodness of the fit due to the different number of parameters characterizing the models that are compared.

The results for the several cases that we study can be found in Figs. 1–6, where also the IC value for each model is reported, and in Tables 2–5 in Appendix A. To begin with, we may look at a fit where we vary only two NP WCs $C_{9,\mu}^{NP}$ and $C_{9,e}^{NP}$, i.e. case (I). According to the IC, this is likely the best-fit scenario we have found, in agreement with previous detailed studies as the one in Ref. [60]. Interestingly, in the PDD approach we get an IC quite significantly lower than the one reported for the PMD approach: this result warmly suggests that a better fit of the data is provided by the former case. This, in fact, is a general trend that we notice in all the scenarios we studied, i.e. larger long-distance contributions than the ones estimated in [78] allow for an overall better description of data. We highlight that this holds even when a New Physics scenario is clearly preferred with respect to the SM limit, i.e. when NP WCs should identically vanish.

This is evident when we look at the IC for the case in which we vary the three NP parameters C_7^{NP} , $C_{10,\mu}^{NP}$ and $C_{10,e}^{NP}$, i.e. case (IV). The model comparison between the PDD and PMD realization of this NP benchmark is indeed quite informative: NP effects in the dipole operator and in the axial semileptonic currents cannot address at the same time R_{K,K^*} ratios and the P_5' anomaly in a satisfactory way when we stick to small non-factorizable QCD power corrections; however, this is no longer true when we allow for a

more conservative estimate of the hadronic uncertainties of the model. In particular, the tension in the fit coming from the angular analysis of $B \rightarrow K^* \mu \mu$ can be now addressed by large QCD effects as those given in Eq. (2.5), while a $C_{10,e} \neq 0$ at 3σ can successfully describe all the observational hints of LFUV showed by current data. To our knowledge, contrary to other scenarios here explored, this interesting possibility of *axial lepton-flavor violating NP* has been overlooked in previous global analyzes [59–62].

It is important to stress that – while larger hadronic contributions accommodate better tensions in the data – the evidence of NP in our fit is always at the 3σ level for one of the semileptonic NP WCs used in the analysis, given the need of a source of LFUV coming mainly from R_{K,K^*} data. In particular, we remark that in the best-fit PMD scenarios of cases (I) and (II) we get evidence for NP at $\sim 7\sigma$. However, looking at the correspondent PDD scenarios, the NP evidence goes back to the 3σ level.

Concerning case (III), we observe very similar findings to the ones obtained for case (I), given the well constrained effective coupling for the radiative dipole operator coming especially from the inclusive $B \rightarrow X_s \gamma$ branching fractions.

In Tables 4–5 (see Appendix A) we report mean and standard deviation for the NP WCs and absolute values of h_λ for all the cases considered in the analysis. It is also relevant to observe that, once we switch on NP effects in order to explain observables like R_{K,K^*} and possibly at the same time also P'_5 , within both the PMD and PDD approach we find small values for $|h_\lambda^{(1,2)}|$, but non-negligible correlation with NP parameters. This result may be to some extent at odd with a global analysis of the angular observables only, where within the PDD approach one may explain everything in terms of hadronic contributions and find an important dependence on the dilepton mass squared of same ones [24]. Therefore, the R_{K,K^*} observables are truly genuine discriminators between this twofold interpretation of the P'_5 anomaly.

Concerning Tables 4–5, we would like to point the attention of the reader to the pattern displayed by the transverse ratios $R_{K^*}^T$ and R_ϕ^T : cases (I)–(III) predict these values to be ~ 1 with narrow error, while the remaining cases "forecast" more relaxed predictions, with case (IV) central values going down to ~ 0.5 . Therefore, obtaining experimental information on transverse ratios may help discerning between the different NP scenarios.

Eventually, we would like to end our discussion with a brief inspection of case (V), defined by varying C_7^{NP} , $C_{9,\mu}^{NP}$, $C_{9,e}^{NP}$ and correlating the semi-leptonic vector and axial currents according to $C_{9,\mu,e}^{NP} = -C_{10,\mu,e}^{NP}$. As we can see from Fig. 5 and Tables 4–5, this model shows a reasonably good agreement with data without requiring any large size for NP WCs in oppositions to all the other previous cases. Moreover, looking at Tables 2–3, we note that this case is the only one where all the ratios lie around a value of ~ 0.7 with appreciably small spread. However, we also performed a more general case in which we introduced a fourth parameter, g_{VA} defined by $C_{10,\mu,e}^{NP} = g_{VA} C_{9,\mu,e}^{NP}$ to investigate a continuum of cases where the two WCs would be correlated. As can be seen in Fig. 6 the best fit to this new parameter sits around 0. In the PMD approach we find that it gives a better fit than what is given by enforcing $C_{9,\mu,e}^{NP} = -C_{10,\mu,e}^{NP}$ by comparing the respective ICs. This case begs for a detailed analysis which we shall leave for a future work [77].

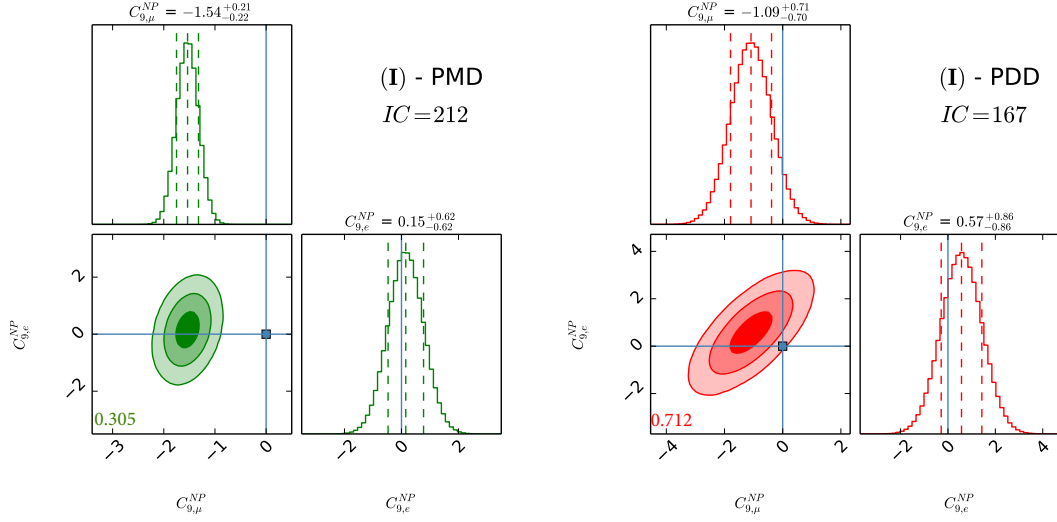


Figure 1. The two NP parameter fit using $C_{9,\mu}^{NP}$ and $C_{9,e}^{NP}$. Here and in the following, the left green panel shows the results for the PMD approach and the right red panel shows that for the PDD one. In the 1D distributions we show the 16th, 50th and 84th percentile marked with the dashed lines. In the correlation plots we show the 1,2 and 3 σ contours in decreasing degrees of transparency. The blue square and lines identify the values of the NP WCs in the SM limit. The numbers at the bottom left corner of the 2D plots refer to the correlation. We also report IC values for the two approaches (see Eqn. 3.1). Preferred models are expected to give smaller IC values.

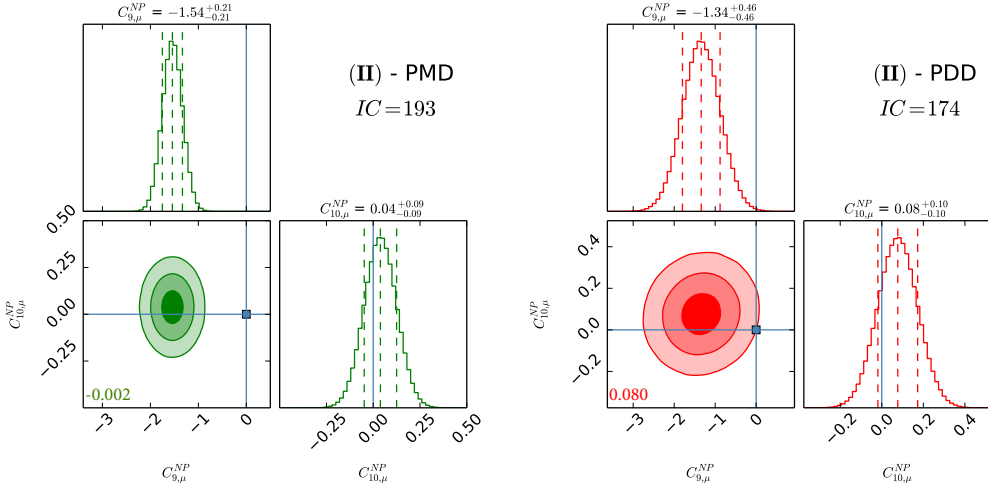


Figure 2. The two NP parameter fit using $C_{9,\mu}^{NP}$ and $C_{10,\mu}^{NP}$. See caption of Fig.1 for the colour coding.

4 Discussion

In this work, we critically examin several BSM scenarios in order to possibly explain the growing pattern of B anomalies, recently enriched by the R_{K^*} measurement performed by

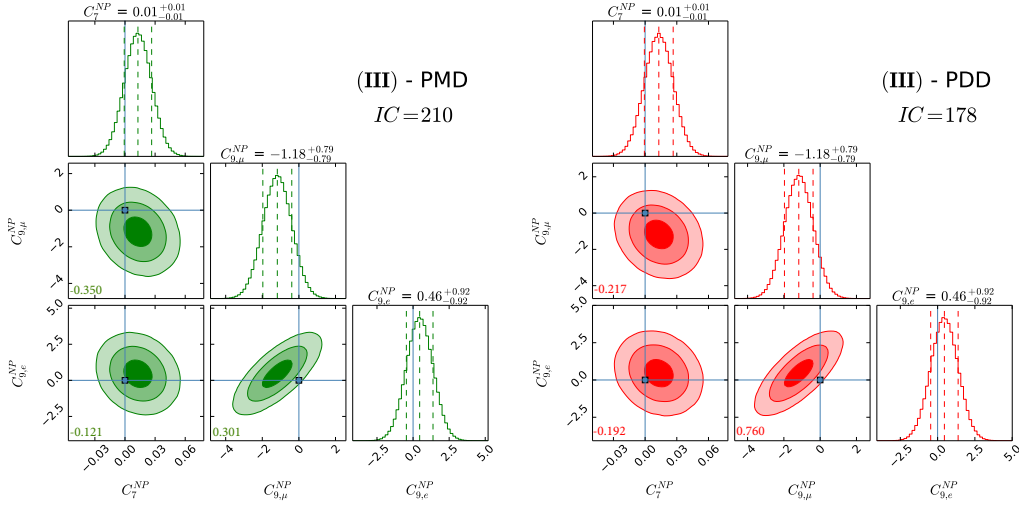


Figure 3. The three NP parameter fit using C_7^{NP} , $C_{9,\mu}^{NP}$ and $C_{9,e}^{NP}$. See caption of Fig.1 for the colour coding.

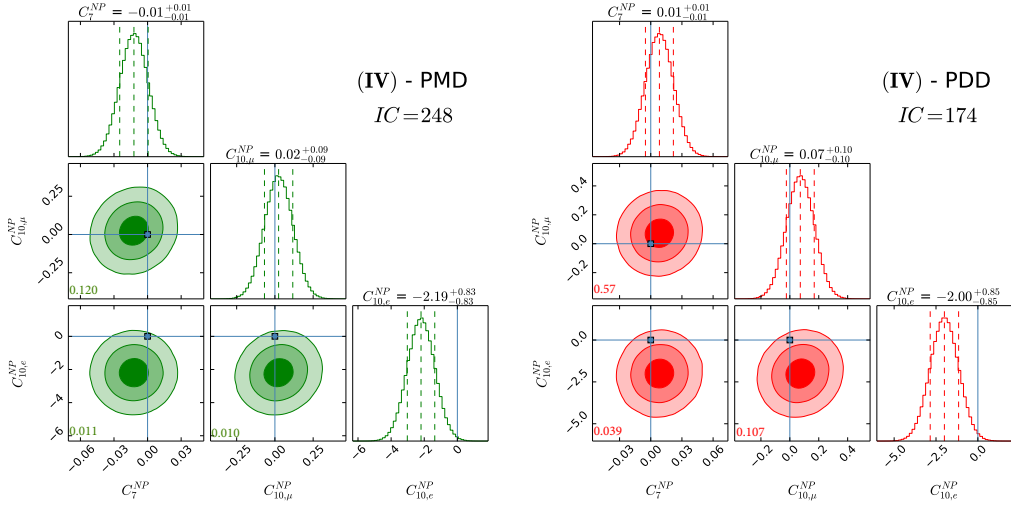


Figure 4. The three NP parameter fit using C_7^{NP} , $C_{10,\mu}^{NP}$ and $C_{10,e}^{NP}$. See caption of Fig.1 for the colour coding.

the LHCb collaboration [66]. We carried out our analysis in an effective field theory framework, describing the non-factorizable power corrections by means of 18 free parameters in our fit along the lines of Ref. [24].

We performed all our fits using two different hadronic models. The first approach, labelled PMD, relies completely on the phenomenological model in [78] and corresponds to the more widely used choice in the literature. The second one, named PDD, imposes the phenomenological model only at $q^2 \leq 1$, in a more conservative way which allows the data to drive the hadronic contributions in the higher invariant mass region.

Regarding the NP contributions we analyze five different benchmark scenarios, differenti-

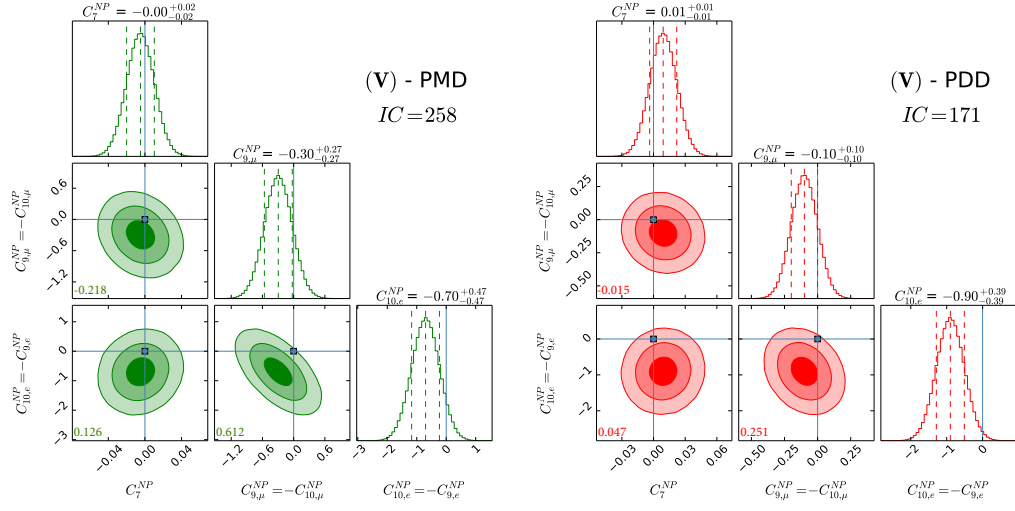


Figure 5. The three NP parameter fit using C_7^{NP} , $C_{9,\mu}^{NP}$, $C_{9,e}^{NP}$ and $C_{10,\mu,e}^{NP} = -C_{9,\mu,e}^{NP}$. See caption of Fig.1 for the colour coding.

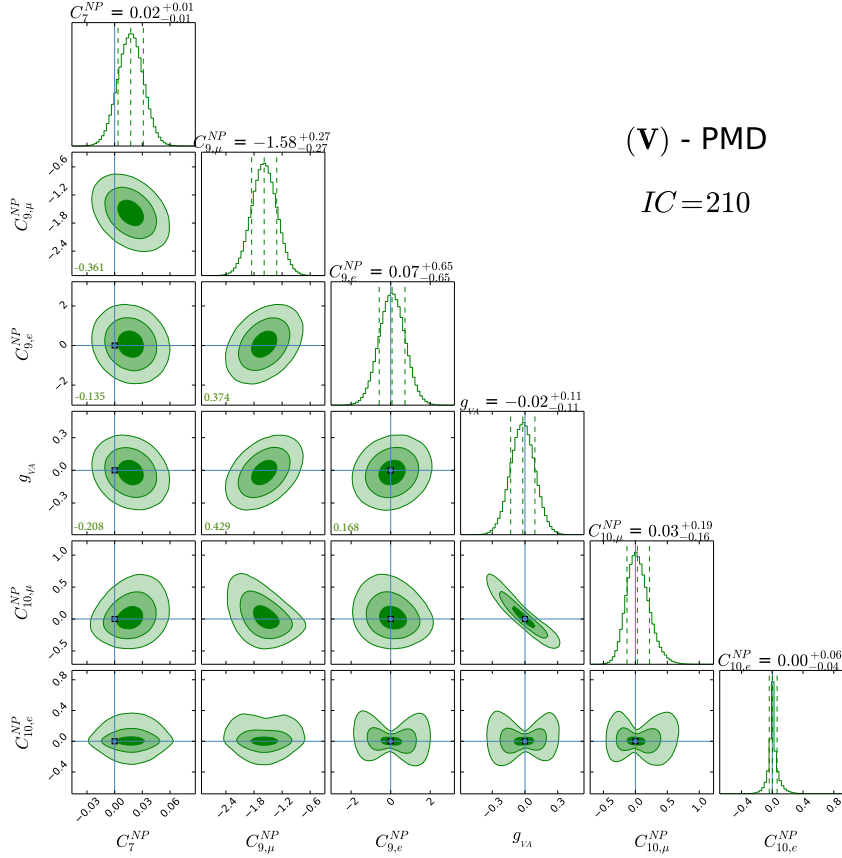


Figure 6. The four NP parameter fit using C_7^{NP} , $C_{9,\mu}^{NP}$, $C_{9,e}^{NP}$ and $C_{10,\mu,e}^{NP} = g_{VA} C_{9,\mu,e}^{NP}$. See caption of Fig.1 for the colour coding.

ated by distinct choices of NP WCs employed in the fits. Case **(I)** allows for $C_{9,\mu}^{NP}$ and $C_{9,e}^{NP}$, while case **(II)** considers the scenario with $C_{9,\mu}^{NP}$ and $C_{10,\mu}^{NP}$; case **(III)** studies NP effects coming as C_7^{NP} , $C_{9,\mu}^{NP}$ and $C_{9,e}^{NP}$, and case **(IV)** is equal to the latter but with C_{10}^{NP} instead of C_9^{NP} . Finally, case **(V)** studies the possibility described in the third case with $C_{10,\mu,e}^{NP} = -C_{9,\mu,e}^{NP}$ enforced. Our main results are effectively collected in Figs. 1-6 and reported also in Tables 2-5.

An important feature that arises from this analysis is a concrete measure of the significance of hadronic contributions while allowing for NP to appear in the observables under consideration. From our results, we see that in general the PDD approach, which allows for a more conservative hadronic model, fits the data much better judging by the ICs of all the scenarios, as compared to PMD which consistently have higher ICs. This leads us to believe that a global fit done in a fashion as in this analysis highlights the relevance of the non-trivial interplay of QCD power corrections with the size of NP effects required by intriguing measurements like R_K and R_{K^*} . Waiting for a possible update of the former, and the compelling measurements of more ratios, such are the ones predicted in Tables 2-3, we wish to stress the challenge on interpreting the shape of NP in light of the original findings of our work.

In particular, from our NP analysis of radiative and (semi-)leptonic B decays, we would like to draw the attention of the reader to:

- A $C_{9,\mu}^{NP}$ and $C_{9,e}^{NP}$ NP scenario is usually corroborated as the most satisfactory and minimal benchmark necessary to explain this set of anomalies. From Fig. 1 we find that a naive $\sim 7\sigma$ evidence in favour of $C_{9,\mu}^{NP} \neq 0$ boils down to only $\sim 3\sigma$ when a more conservative approach on hadronic effects is taken into account.
- A C_7^{NP} , $C_{10,\mu}^{NP}$ and $C_{10,e}^{NP}$ NP scenario can be employed to explain the set of anomalies. To our knowledge, NP axial currents have been usually overlooked in the literature. However, this is actually an interesting case: on the one hand it displays the worst IC between all PMD fits, as shown in Fig. 4; on the other hand, when the more conservative approach of hadronic contribution is considered, we found that this scenario is equally capable of explaining the data, with an IC comparable to the one for the widely analyzed $C_{9,\mu}^{NP}$ and $C_{9,e}^{NP}$ NP scenario.

In conclusion, while our global analysis confirms the need of NP sources to fully explain the current experimental situation in B physics, it clearly delineates the challenges and the subtleties present in the attempt to quantify the size and to identify the pattern of the underlying BSM theory addressing the current experimental situation.

Acknowledgments

The research leading to these results has received funding from the European Research Council under the European Union’s Seventh Framework Programme (FP/2007-2013) / ERC Grant Agreements n. 279972 “NPFlavour” and n. 267985 “DaMeSyFla”. We bless Alfredo Urbano for invaluable correspondence within and beyond the flavour of New Physics.

A Tables

In this section we report the tables with results obtained from our fits. In Table 2 we list the PDD results obtained for the key observables in the five NP scenarios. Analogous results for the PMD approach can be found in Table 3. Mean and standard deviation for the NP WCs and h_λ absolute values are reported in Table 4 for the PDD approach and in Table 5 for the PMD one.

Obs.	Exp. value	(I)	(II)	(III)	(IV)	(V)
R_K	0.753 ± 0.090	0.783 ± 0.07	0.811 ± 0.06	0.784 ± 0.07	0.879 ± 0.052	0.801 ± 0.067
R_{K^*}	0.707 ± 0.102	0.781 ± 0.084	0.807 ± 0.065	0.783 ± 0.084	0.57 ± 0.12	0.658 ± 0.099
$R_{K^*}^L$	—	0.703 ± 0.096	0.736 ± 0.078	0.707 ± 0.096	0.58 ± 0.12	0.64 ± 0.11
$R_{K^*}^T$	—	1.03 ± 0.047	1.024 ± 0.043	1.026 ± 0.048	0.54 ± 0.13	0.73 ± 0.11
R_ϕ	—	0.757 ± 0.088	0.786 ± 0.068	0.76 ± 0.088	0.58 ± 0.12	0.65 ± 0.1
R_ϕ^L	—	0.699 ± 0.096	0.732 ± 0.078	0.703 ± 0.096	0.58 ± 0.12	0.62 ± 0.11
R_ϕ^T	—	1.021 ± 0.05	1.017 ± 0.044	1.018 ± 0.05	0.55 ± 0.13	0.74 ± 0.1
$P_{5\text{LHCb}}^{[4,6]}$	-0.301 ± 0.160	-0.404 ± 0.069	-0.399 ± 0.071	-0.406 ± 0.069	-0.437 ± 0.069	-0.396 ± 0.098
$P_{5\text{LHCb}}^{[6,8]}$	-0.505 ± 0.124	-0.529 ± 0.082	-0.532 ± 0.084	-0.53 ± 0.082	-0.532 ± 0.081	-0.482 ± 0.095
$P_{5\text{ATLAS}}^{[4,6]}$	-0.26 ± 0.39	-0.404 ± 0.069	-0.399 ± 0.071	-0.406 ± 0.069	-0.437 ± 0.069	-0.396 ± 0.098
$P_{5\text{CMS}}^{[4,3,6]}$	-0.955 ± 0.268	-0.42 ± 0.07	-0.416 ± 0.071	-0.422 ± 0.069	-0.45 ± 0.069	-0.408 ± 0.097
$P_{5\text{CMS}}^{[6,8,68]}$	-0.660 ± 0.220	-0.539 ± 0.087	-0.543 ± 0.09	-0.54 ± 0.088	-0.54 ± 0.086	-0.49 ± 0.1
$P_{5\text{BELLE}}^{[4,8]}$	-0.025 ± 0.318	-0.472 ± 0.071	-0.472 ± 0.071	-0.473 ± 0.07	-0.488 ± 0.069	-0.441 ± 0.085
$P_{5,e\text{BELLE}}^{[4,8]}$	-0.510 ± 0.272	-0.741 ± 0.084	-0.707 ± 0.081	-0.745 ± 0.084	-0.383 ± 0.065	-0.609 ± 0.075

Table 2. Experimental results (with symmetrized errors) and results from the fit for key observables in the PDD approach. See Sec. 2.1 for details on the five NP scenarios.

Obs.	Exp. value	(I)	(II)	(III)	(IV)	(V)
R_K	0.753 ± 0.090	0.775 ± 0.067	0.785 ± 0.027	0.776 ± 0.069	0.868 ± 0.051	0.825 ± 0.06
R_{K^*}	0.707 ± 0.102	0.776 ± 0.083	0.786 ± 0.035	0.78 ± 0.083	0.55 ± 0.11	0.65 ± 0.1
$R_{K^*}^L$	—	0.696 ± 0.094	0.704 ± 0.04	0.7 ± 0.095	0.57 ± 0.11	0.64 ± 0.1
$R_{K^*}^T$	—	1.035 ± 0.042	1.042 ± 0.04	1.031 ± 0.041	0.51 ± 0.12	0.703 ± 0.096
R_ϕ	—	0.755 ± 0.086	0.765 ± 0.036	0.758 ± 0.087	0.56 ± 0.11	0.65 ± 0.1
R_ϕ^L	—	0.695 ± 0.094	0.703 ± 0.039	0.699 ± 0.095	0.58 ± 0.11	0.64 ± 0.1
R_ϕ^T	—	1.029 ± 0.044	1.037 ± 0.039	1.026 ± 0.043	0.51 ± 0.12	0.697 ± 0.097
$P_{5\text{LHCb}}^{[4,6]}$	-0.301 ± 0.160	-0.42 ± 0.059	-0.419 ± 0.058	-0.415 ± 0.058	-0.677 ± 0.039	-0.662 ± 0.038
$P_{5\text{LHCb}}^{[6,8]}$	-0.505 ± 0.124	-0.601 ± 0.067	-0.605 ± 0.063	-0.587 ± 0.067	-0.793 ± 0.038	-0.782 ± 0.04
$P_{5\text{ATLAS}}^{[4,6]}$	-0.26 ± 0.39	-0.42 ± 0.059	-0.419 ± 0.058	-0.415 ± 0.058	-0.677 ± 0.039	-0.662 ± 0.038
$P_{5\text{CMS}}^{[4,3,6]}$	-0.955 ± 0.268	-0.441 ± 0.058	-0.44 ± 0.057	-0.435 ± 0.057	-0.694 ± 0.038	-0.679 ± 0.037
$P_{5\text{CMS}}^{[6,8,68]}$	-0.660 ± 0.220	-0.618 ± 0.073	-0.623 ± 0.067	-0.603 ± 0.074	-0.798 ± 0.041	-0.786 ± 0.044
$P_{5\text{BELLE}}^{[4,8]}$	-0.025 ± 0.318	-0.518 ± 0.056	-0.52 ± 0.056	-0.508 ± 0.056	-0.738 ± 0.035	-0.725 ± 0.035
$P_{5,e\text{BELLE}}^{[4,8]}$	-0.510 ± 0.272	-0.799 ± 0.061	-0.802 ± 0.029	-0.794 ± 0.066	-0.587 ± 0.059	-0.783 ± 0.032

Table 3. Experimental results (with symmetrized errors) and results from the fit for key observables in the PMD approach. See Sec. 2.1 for details on the five NP scenarios.

Par.	(I)	(II)	(III)	(IV)	(V)
C_7^{NP}	—	—	0.013 ± 0.014	0.008 ± 0.014	0.06 ± 0.16
$C_{9,\mu}^{\text{NP}}$	-1.09 ± 0.71	-1.34 ± 0.46	-1.18 ± 0.79	—	-0.87 ± 0.83
$C_{9,e}^{\text{NP}}$	0.57 ± 0.86	—	0.46 ± 0.93	—	0.22 ± 0.82
$C_{10,\mu}^{\text{NP}}$	—	0.077 ± 0.096	—	0.072 ± 0.097	0.87 ± 0.83
$C_{10,e}^{\text{NP}}$	—	—	—	-2 ± 0.85	-0.22 ± 0.82
$ h_0^{(0)} \cdot 10^4$	1.9 ± 1.2	2.1 ± 1.3	1.9 ± 1.3	1.5 ± 1.2	2.5 ± 2
$ h_+^{(0)} \cdot 10^4$	0.076 ± 0.067	0.079 ± 0.068	0.079 ± 0.072	0.085 ± 0.073	0.1 ± 0.1
$ h_-^{(0)} \cdot 10^4$	0.53 ± 0.21	0.54 ± 0.21	0.53 ± 0.21	0.58 ± 0.23	0.78 ± 0.66
$ h_0^{(1)} \cdot 10^4$	1.5 ± 1.4	1.9 ± 1.6	1.8 ± 1.5	1.6 ± 1.3	3.3 ± 2.8
$ h_+^{(1)} \cdot 10^4$	0.41 ± 0.31	0.41 ± 0.3	0.39 ± 0.29	0.4 ± 0.3	0.44 ± 0.32
$ h_-^{(1)} \cdot 10^4$	0.49 ± 0.36	0.51 ± 0.38	0.52 ± 0.37	0.74 ± 0.45	1 ± 1
$ h_0^{(2)} \cdot 10^4$	0.22 ± 0.19	0.26 ± 0.23	0.26 ± 0.21	0.21 ± 0.18	0.38 ± 0.35
$ h_+^{(2)} \cdot 10^4$	0.135 ± 0.09	0.137 ± 0.091	0.122 ± 0.083	0.127 ± 0.089	0.17 ± 0.14
$ h_-^{(2)} \cdot 10^4$	0.134 ± 0.095	0.123 ± 0.094	0.141 ± 0.095	0.199 ± 0.093	0.23 ± 0.14

Table 4. Results from the fit for WCs and hadronic contributions in the PDD approach. See Sec. 2.1 for details on the five NP scenarios.

Par.	(I)	(II)	(III)	(IV)	(V)
C_7^{NP}	—	—	0.018 ± 0.013	-0.012 ± 0.013	-0.007 ± 0.013
$C_{9,\mu}^{\text{NP}}$	-1.54 ± 0.22	-1.54 ± 0.21	-1.65 ± 0.23	—	-0.23 ± 0.13
$C_{9,e}^{\text{NP}}$	0.15 ± 0.63	—	0.02 ± 0.63	—	0.75 ± 0.41
$C_{10,\mu}^{\text{NP}}$	—	0.038 ± 0.087	—	0.025 ± 0.093	0.23 ± 0.13
$C_{10,e}^{\text{NP}}$	—	—	—	-2.2 ± 0.83	-0.75 ± 0.41
$ h_0^{(0)} \cdot 10^4$	2.3 ± 1.7	2.2 ± 1.5	2.6 ± 1.9	1.8 ± 1.5	1.9 ± 1.7
$ h_+^{(0)} \cdot 10^4$	0.07 ± 0.056	0.073 ± 0.059	0.072 ± 0.062	0.072 ± 0.057	0.073 ± 0.061
$ h_-^{(0)} \cdot 10^4$	0.52 ± 0.15	0.51 ± 0.14	0.5 ± 0.14	0.51 ± 0.15	0.51 ± 0.14
$ h_0^{(1)} \cdot 10^4$	1.9 ± 1.8	1.7 ± 1.6	2.1 ± 2	1.6 ± 1.4	1.6 ± 1.5
$ h_+^{(1)} \cdot 10^4$	0.14 ± 0.13	0.13 ± 0.13	0.19 ± 0.18	0.12 ± 0.12	0.17 ± 0.17
$ h_-^{(1)} \cdot 10^4$	0.29 ± 0.29	0.25 ± 0.24	0.24 ± 0.22	0.33 ± 0.25	0.3 ± 0.21
$ h_0^{(2)} \cdot 10^4$	0.29 ± 0.27	0.26 ± 0.24	0.32 ± 0.3	0.23 ± 0.23	0.24 ± 0.23
$ h_+^{(2)} \cdot 10^4$	0.03 ± 0.027	0.028 ± 0.028	0.04 ± 0.038	0.025 ± 0.024	0.034 ± 0.035
$ h_-^{(2)} \cdot 10^4$	0.052 ± 0.051	0.045 ± 0.043	0.04 ± 0.038	0.058 ± 0.046	0.05 ± 0.039

Table 5. Results from the fit for WCs and hadronic contributions in the PMD approach. See Sec. 2.1 for details on the five NP scenarios.

References

- [1] N. Cabibbo, *Unitary Symmetry and Leptonic Decays*, *Phys. Rev. Lett.* **10** (1963) 531–533.
- [2] Y. Amhis et al., *Averages of b -hadron, c -hadron, and τ -lepton properties as of summer 2016*, [arXiv:1612.07233](#).
- [3] A. J. Buras, *Climbing NLO and NNLO Summits of Weak Decays*, [arXiv:1102.5650](#).

- [4] F. Beaujean, C. Bobeth, and D. van Dyk, *Comprehensive Bayesian analysis of rare (semi)leptonic and radiative B decays*, *Eur.Phys.J.* **C74** (2014), no. 6 2897, [[arXiv:1310.2478](#)].
- [5] T. Blake, G. Lanfranchi, and D. M. Straub, *Rare B Decays as Tests of the Standard Model*, *Prog. Part. Nucl. Phys.* **92** (2017) 50–91, [[arXiv:1606.00916](#)].
- [6] S. L. Glashow, J. Iliopoulos, and L. Maiani, *Weak Interactions with Lepton-Hadron Symmetry*, *Phys. Rev.* **D2** (1970) 1285–1292.
- [7] **Belle** Collaboration, T. Saito et al., *Measurement of the $\bar{B} \rightarrow X_s \gamma$ Branching Fraction with a Sum of Exclusive Decays*, *Phys. Rev.* **D91** (2015), no. 5 052004, [[arXiv:1411.7198](#)].
- [8] **Belle** Collaboration, A. Abdesselam et al., *Measurement of the inclusive $B \rightarrow X_{s+d} \gamma$ branching fraction, photon energy spectrum and HQE parameters*, in *Proceedings, 38th International Conference on High Energy Physics (ICHEP 2016): Chicago, IL, USA, August 3-10, 2016*, 2016. [arXiv:1608.02344](#).
- [9] **BaBar** Collaboration, J. P. Lees et al., *Precision Measurement of the $B \rightarrow X_s \gamma$ Photon Energy Spectrum, Branching Fraction, and Direct CP Asymmetry $A_{CP}(B \rightarrow X_{s+d} \gamma)$* , *Phys. Rev. Lett.* **109** (2012) 191801, [[arXiv:1207.2690](#)].
- [10] **LHCb** Collaboration, R. Aaij et al., *Differential branching fraction and angular analysis of the decay $B^0 \rightarrow K^{*0} \mu^+ \mu^-$* , *JHEP* **08** (2013) 131, [[arXiv:1304.6325](#)].
- [11] **LHCb** Collaboration, *Angular analysis of the $B^0 \rightarrow K^{*0} \mu^+ \mu^-$ decay*, *LHCb-CONF-2015-002, CERN-LHCb-CONF-2015-002* (2015).
- [12] T. Blake, M. Gersabeck, L. Hofer, S. Jäger, Z. Liu, and R. Zwicky, *Round table: Flavour anomalies in $b \rightarrow sl^+ l^-$ processes*, *EPJ Web Conf.* **137** (2017) 01001, [[arXiv:1703.10005](#)].
- [13] J. Matias, F. Mescia, M. Ramon, and J. Virto, *Complete Anatomy of $\bar{B}_d \rightarrow \bar{K}^{*0}(\rightarrow K \pi) l^+ l^-$ and its angular distribution*, *JHEP* **1204** (2012) 104, [[arXiv:1202.4266](#)].
- [14] S. Descotes-Genon, J. Matias, M. Ramon, and J. Virto, *Implications from clean observables for the binned analysis of $B \rightarrow K^* \mu^+ \mu^-$ at large recoil*, *JHEP* **1301** (2013) 048, [[arXiv:1207.2753](#)].
- [15] S. Descotes-Genon, T. Hurth, J. Matias, and J. Virto, *Optimizing the basis of $B \rightarrow K^* \ell^+ \ell^-$ observables in the full kinematic range*, *JHEP* **1305** (2013) 137, [[arXiv:1303.5794](#)].
- [16] J. Matias and N. Serra, *Symmetry relations between angular observables in $B^0 \rightarrow K^* \mu^+ \mu^-$ and the LHCb P'_5 anomaly*, *Phys. Rev.* **D90** (2014), no. 3 034002, [[arXiv:1402.6855](#)].
- [17] **LHCb** Collaboration, R. Aaij et al., *Measurement of Form-Factor-Independent Observables in the Decay $B^0 \rightarrow K^{*0} \mu^+ \mu^-$* , *Phys.Rev.Lett.* **111** (2013), no. 19 191801, [[arXiv:1308.1707](#)].
- [18] **LHCb** Collaboration, R. Aaij et al., *Angular analysis of the $B^0 \rightarrow K^{*0} \mu^+ \mu^-$ decay using 3 fb^{-1} of integrated luminosity*, *JHEP* **02** (2016) 104, [[arXiv:1512.04442](#)].
- [19] **Belle** Collaboration, A. Abdesselam et al., *Angular analysis of $B^0 \rightarrow K^*(892)^0 \ell^+ \ell^-$* , in *Proceedings, LHCSki 2016 - A First Discussion of 13 TeV Results: Obergurgl, Austria, April 10-15, 2016*, 2016. [arXiv:1604.04042](#).
- [20] S. Descotes-Genon, L. Hofer, J. Matias, and J. Virto, *On the impact of power corrections in the prediction of $B \rightarrow K^* \mu^+ \mu^-$ observables*, *JHEP* **1412** (2014) 125, [[arXiv:1407.8526](#)].

- [21] S. Jäger and J. Martin Camalich, *On $B \rightarrow V\ell\ell$ at small dilepton invariant mass, power corrections, and new physics*, *JHEP* **1305** (2013) 043, [[arXiv:1212.2263](#)].
- [22] S. Jäger and J. Martin Camalich, *Reassessing the discovery potential of the $B \rightarrow K^*\ell^+\ell^-$ decays in the large-recoil region: SM challenges and BSM opportunities*, [arXiv:1412.3183](#).
- [23] J. Lyon and R. Zwicky, *Resonances gone topsy turvy - the charm of QCD or new physics in $b \rightarrow s\ell^+\ell^-$?*, [arXiv:1406.0566](#).
- [24] M. Ciuchini, M. Fedele, E. Franco, S. Mishima, A. Paul, L. Silvestrini, and M. Valli, *$B \rightarrow K^*\ell^+\ell^-$ decays at large recoil in the Standard Model: a theoretical reappraisal*, *JHEP* **06** (2016) 116, [[arXiv:1512.07157](#)].
- [25] T. Hurth, F. Mahmoudi, and S. Neshatpour, *On the anomalies in the latest LHCb data*, *Nucl. Phys.* **B909** (2016) 737–777, [[arXiv:1603.00865](#)].
- [26] J. Martin Camalich, *Hadronic uncertainties in semileptonic B decays*, *PoS BEAUTY2016* (2016) 037.
- [27] M. Ciuchini, M. Fedele, E. Franco, S. Mishima, A. Paul, L. Silvestrini, and M. Valli, *$B \rightarrow K^*\ell^+\ell^-$ in the Standard Model: Elaborations and Interpretations*, in *Proceedings, 38th International Conference on High Energy Physics (ICHEP 2016): Chicago, IL, USA, August 3-10, 2016*, 2016. [arXiv:1611.04338](#).
- [28] B. Capdevila, S. Descotes-Genon, L. Hofer, and J. Matias, *Hadronic uncertainties in $B \rightarrow K^*\mu^+\mu^-$: a state-of-the-art analysis*, *JHEP* **04** (2017) 016, [[arXiv:1701.08672](#)].
- [29] **ATLAS** Collaboration, *Angular analysis of $B_d^0 \rightarrow K^*\mu^+\mu^-$ decays in pp collisions at $\sqrt{s} = 8$ TeV with the ATLAS detector*, Tech. Rep. ATLAS-CONF-2017-023, CERN, Geneva, Apr, 2017.
- [30] **CMS** Collaboration, *Measurement of the P_1 and P'_5 angular parameters of the decay $B^0 \rightarrow K^{*0}\mu^+\mu^-$ in proton-proton collisions at $\sqrt{s} = 8$ TeV*, Tech. Rep. CMS-PAS-BPH-15-008, CERN, Geneva, 2017.
- [31] **LHCb** Collaboration, R. Aaij et al., *Differential branching fractions and isospin asymmetries of $B \rightarrow K^{(*)}\mu^+\mu^-$ decays*, *JHEP* **06** (2014) 133, [[arXiv:1403.8044](#)].
- [32] **LHCb** Collaboration, R. Aaij et al., *Angular analysis and differential branching fraction of the decay $B_s^0 \rightarrow \phi\mu^+\mu^-$* , *JHEP* **09** (2015) 179, [[arXiv:1506.08777](#)].
- [33] A. Khodjamirian, T. Mannel, and Y. M. Wang, *$B \rightarrow K\ell^+\ell^-$ decay at large hadronic recoil*, *JHEP* **02** (2013) 010, [[arXiv:1211.0234](#)].
- [34] **LHCb** Collaboration, R. Aaij et al., *Measurement of the phase difference between short- and long-distance amplitudes in the $B^+ \rightarrow K^+\mu^+\mu^-$ decay*, *Eur. Phys. J.* **C77** (2017) 161, [[arXiv:1612.06764](#)].
- [35] **LHCb** Collaboration, R. Aaij et al., *Test of lepton universality using $B^+ \rightarrow K^+\ell^+\ell^-$ decays*, *Phys. Rev. Lett.* **113** (2014) 151601, [[arXiv:1406.6482](#)].
- [36] M. Bordone, G. Isidori, and A. Pattori, *On the Standard Model predictions for R_K and R_{K^*}* , *Eur. Phys. J.* **C76** (2016), no. 8 440, [[arXiv:1605.07633](#)].
- [37] R. Alonso, B. Grinstein, and J. Martin Camalich, *$SU(2) \times U(1)$ gauge invariance and the shape of new physics in rare B decays*, *Phys. Rev. Lett.* **113** (2014) 241802, [[arXiv:1407.7044](#)].

- [38] G. Hiller and M. Schmaltz, *R_K and future $b \rightarrow s\ell\ell$ physics beyond the standard model opportunities*, *Phys. Rev.* **D90** (2014) 054014, [[arXiv:1408.1627](#)].
- [39] S. L. Glashow, D. Guadagnoli, and K. Lane, *Lepton Flavor Violation in B Decays?*, *Phys. Rev. Lett.* **114** (2015) 091801, [[arXiv:1411.0565](#)].
- [40] G. Hiller and M. Schmaltz, *Diagnosing lepton-nonuniversality in $b \rightarrow s\ell\ell$* , *JHEP* **02** (2015) 055, [[arXiv:1411.4773](#)].
- [41] B. Gripaios, M. Nardecchia, and S. A. Renner, *Composite leptoquarks and anomalies in B -meson decays*, *JHEP* **05** (2015) 006, [[arXiv:1412.1791](#)].
- [42] A. Crivellin, G. D'Ambrosio, and J. Heeck, *Addressing the LHC flavor anomalies with horizontal gauge symmetries*, *Phys. Rev.* **D91** (2015), no. 7 075006, [[arXiv:1503.03477](#)].
- [43] A. Crivellin, L. Hofer, J. Matias, U. Nierste, S. Pokorski, and J. Rosiek, *Lepton-flavour violating B decays in generic Z' models*, *Phys. Rev.* **D92** (2015), no. 5 054013, [[arXiv:1504.07928](#)].
- [44] A. Celis, J. Fuentes-Martin, M. Jung, and H. Serodio, *Family nonuniversal $Z\bar{A}\bar{A}s$ models with protected flavor-changing interactions*, *Phys. Rev.* **D92** (2015), no. 1 015007, [[arXiv:1505.03079](#)].
- [45] R. Alonso, B. Grinstein, and J. Martin Camalich, *Lepton universality violation and lepton flavor conservation in B -meson decays*, *JHEP* **10** (2015) 184, [[arXiv:1505.05164](#)].
- [46] A. Greljo, G. Isidori, and D. Marzocca, *On the breaking of Lepton Flavor Universality in B decays*, *JHEP* **07** (2015) 142, [[arXiv:1506.01705](#)].
- [47] L. Calibbi, A. Crivellin, and T. Ota, *Effective Field Theory Approach to $b \rightarrow s\ell\ell^{(\prime)}$, $B \rightarrow K^{(*)}\nu\bar{\nu}$ and $B \rightarrow D^{(*)}\tau\nu$ with Third Generation Couplings*, *Phys. Rev. Lett.* **115** (2015) 181801, [[arXiv:1506.02661](#)].
- [48] A. Falkowski, M. Nardecchia, and R. Ziegler, *Lepton Flavor Non-Universality in B -meson Decays from a $U(2)$ Flavor Model*, *JHEP* **11** (2015) 173, [[arXiv:1509.01249](#)].
- [49] C.-W. Chiang, X.-G. He, and G. Valencia, *Z model for $b \rightarrow s\ell\bar{\ell}$ flavor anomalies*, *Phys. Rev.* **D93** (2016), no. 7 074003, [[arXiv:1601.07328](#)].
- [50] D. Becirevic, O. Sumensari, and R. Zukanovich Funchal, *Lepton flavor violation in exclusive $b \rightarrow s$ decays*, *Eur. Phys. J.* **C76** (2016), no. 3 134, [[arXiv:1602.00881](#)].
- [51] F. Feruglio, P. Paradisi, and A. Pattori, *Revisiting Lepton Flavor Universality in B Decays*, *Phys. Rev. Lett.* **118** (2017), no. 1 011801, [[arXiv:1606.00524](#)].
- [52] D. Becirevic, N. KoÅanik, O. Sumensari, and R. Zukanovich Funchal, *Palatable Leptoquark Scenarios for Lepton Flavor Violation in Exclusive $b \rightarrow s\ell_1\ell_2$ modes*, *JHEP* **11** (2016) 035, [[arXiv:1608.07583](#)].
- [53] R. Alonso, E. Fernandez Martinez, M. B. Gavela, B. Grinstein, L. Merlo, and P. Quilez, *Gauged Lepton Flavour*, *JHEP* **12** (2016) 119, [[arXiv:1609.05902](#)].
- [54] G. Hiller, D. Loose, and K. Schonwald, *Leptoquark Flavor Patterns & B Decay Anomalies*, *JHEP* **12** (2016) 027, [[arXiv:1609.08895](#)].
- [55] I. Galon, A. Kwa, and P. Tanedo, *Lepton-Flavor Violating Mediators*, *JHEP* **03** (2017) 064, [[arXiv:1610.08060](#)].
- [56] A. Crivellin, J. Fuentes-Martin, A. Greljo, and G. Isidori, *Lepton Flavor Non-Universality in B decays from Dynamical Yukawas*, *Phys. Lett.* **B766** (2017) 77–85, [[arXiv:1611.02703](#)].

- [57] P. Cox, A. Kusenko, O. Sumensari, and T. T. Yanagida, *SU(5) Unification with TeV-scale Leptoquarks*, *JHEP* **03** (2017) 035, [[arXiv:1612.03923](#)].
- [58] T. Hurth and F. Mahmoudi, *On the LHCb anomaly in $B \rightarrow K^* \ell^+ \ell^-$* , *JHEP* **1404** (2014) 097, [[arXiv:1312.5267](#)].
- [59] W. Altmannshofer and D. M. Straub, *New physics in $b \rightarrow s$ transitions after LHC run 1*, *Eur. Phys. J.* **C75** (2015), no. 8 382, [[arXiv:1411.3161](#)].
- [60] S. Descotes-Genon, L. Hofer, J. Matias, and J. Virto, *Global analysis of $b \rightarrow s \ell \ell$ anomalies*, [[arXiv:1510.04239](#)].
- [61] V. G. Chobanova, T. Hurth, F. Mahmoudi, D. Martinez Santos, and S. Neshatpour, *Large hadronic power corrections or new physics in the rare decay $B \rightarrow K^* \ell \ell$?*, [[arXiv:1702.02234](#)].
- [62] W. Altmannshofer, C. Niehoff, P. Stangl, and D. M. Straub, *Status of the $B \rightarrow K^* \mu^+ \mu^-$ anomaly after Moriond 2017*, [[arXiv:1703.09189](#)].
- [63] B. Capdevila, S. Descotes-Genon, J. Matias, and J. Virto, *Assessing lepton-flavour non-universality from $B \rightarrow K^* \ell \ell$ angular analyses*, *JHEP* **10** (2016) 075, [[arXiv:1605.03156](#)].
- [64] N. Serra, R. Silva Coutinho, and D. van Dyk, *Measuring the breaking of lepton flavor universality in $B \rightarrow K^* \ell^+ \ell^-$* , *Phys. Rev.* **D95** (2017), no. 3 035029, [[arXiv:1610.08761](#)].
- [65] Belle Collaboration, S. Wehle et al., *Lepton-Flavor-Dependent Angular Analysis of $B \rightarrow K^* \ell^+ \ell^-$* , *Phys. Rev. Lett.* **118** (2017), no. 11 111801, [[arXiv:1612.05014](#)].
- [66] LHCb Collaboration, S. Bifani, “Search for new physics with $b \rightarrow s \ell^+ \ell^-$ decays at LHCb.” <https://indico.cern.ch/event/580620/>.
- [67] G. Buchalla, A. J. Buras, and M. E. Lautenbacher, *Weak decays beyond leading logarithms*, *Rev. Mod. Phys.* **68** (1996) 1125–1144, [[hep-ph/9512380](#)].
- [68] M. Ciuchini, E. Franco, G. Martinelli, and L. Reina, *The Delta S = 1 effective Hamiltonian including next-to-leading order QCD and QED corrections*, *Nucl. Phys.* **B415** (1994) 403–462, [[hep-ph/9304257](#)].
- [69] K. G. Chetyrkin, M. Misiak, and M. Munz, *$|\Delta F| = 1$ nonleptonic effective Hamiltonian in a simpler scheme*, *Nucl. Phys.* **B520** (1998) 279–297, [[hep-ph/9711280](#)].
- [70] C. Bobeth, M. Misiak, and J. Urban, *Photonic penguins at two loops and $m(t)$ dependence of $BR[B \rightarrow X(s) \ell \ell]$* , *Nucl. Phys.* **B574** (2000) 291–330, [[hep-ph/9910220](#)].
- [71] P. Gambino and U. Haisch, *Complete electroweak matching for radiative B decays*, *JHEP* **10** (2001) 020, [[hep-ph/0109058](#)].
- [72] M. Misiak and M. Steinhauser, *Three loop matching of the dipole operators for $b \rightarrow s \gamma$ and $b \rightarrow sg$* , *Nucl. Phys.* **B683** (2004) 277–305, [[hep-ph/0401041](#)].
- [73] C. Bobeth, P. Gambino, M. Gorbahn, and U. Haisch, *Complete NNLO QCD analysis of $\bar{B} \rightarrow X(s) \ell^+ \ell^-$ and higher order electroweak effects*, *JHEP* **0404** (2004) 071, [[hep-ph/0312090](#)].
- [74] P. Gambino, M. Gorbahn, and U. Haisch, *Anomalous dimension matrix for radiative and rare semileptonic B decays up to three loops*, *Nucl. Phys.* **B673** (2003) 238–262, [[hep-ph/0306079](#)].

- [75] T. Huber, E. Lunghi, M. Misiak, and D. Wyler, *Electromagnetic logarithms in anti- $B \rightarrow X(s) l^+ l^-$* , *Nucl.Phys.* **B740** (2006) 105–137, [[hep-ph/0512066](#)].
- [76] J. Aebischer, A. Crivellin, M. Fael, and C. Greub, *Matching of gauge invariant dimension-six operators for $b \rightarrow s$ and $b \rightarrow c$ transitions*, *JHEP* **05** (2016) 037, [[arXiv:1512.02830](#)].
- [77] M. Ciuchini, A. M. Coutinho, M. Fedele, E. Franco, A. Paul, L. Silvestrini, and M. Valli, *in preparation*.
- [78] A. Khodjamirian, T. Mannel, A. Pivovarov, and Y.-M. Wang, *Charm-loop effect in $B \rightarrow K^{(*)} \ell^+ \ell^-$ and $B \rightarrow K^* \gamma$* , *JHEP* **1009** (2010) 089, [[arXiv:1006.4945](#)].
- [79] M. Beneke, T. Feldmann, and D. Seidel, *Systematic approach to exclusive $B \rightarrow V l^+ l^-$, V gamma decays*, *Nucl.Phys.* **B612** (2001) 25–58, [[hep-ph/0106067](#)].
- [80] A. L. Kagan and M. Neubert, *Isospin breaking in $B \rightarrow K^* \gamma$ decays*, *Phys. Lett.* **B539** (2002) 227–234, [[hep-ph/0110078](#)].
- [81] T. Feldmann and J. Matias, *Forward backward and isospin asymmetry for $B \rightarrow K^* \ell^+ \ell^-$ decay in the standard model and in supersymmetry*, *JHEP* **0301** (2003) 074, [[hep-ph/0212158](#)].
- [82] M. Beneke, T. Feldmann, and D. Seidel, *Exclusive radiative and electroweak $b \rightarrow d$ and $b \rightarrow s$ penguin decays at NLO*, *Eur. Phys. J.* **C41** (2005) 173–188, [[hep-ph/0412400](#)].
- [83] P. Ball, G. W. Jones, and R. Zwicky, *$B \rightarrow V \gamma$ beyond QCD factorisation*, *Phys. Rev.* **D75** (2007) 054004, [[hep-ph/0612081](#)].
- [84] M. Dimou, J. Lyon, and R. Zwicky, *Exclusive Chromomagnetism in heavy-to-light FCNCs*, *Phys. Rev.* **D87** (2013), no. 7 074008, [[arXiv:1212.2242](#)].
- [85] J. Lyon and R. Zwicky, *Isospin asymmetries in $B \rightarrow (K^*, \rho) \gamma / l^+ l^-$ and $B \rightarrow K l^+ l^-$ in and beyond the standard model*, *Phys. Rev.* **D88** (2013), no. 9 094004, [[arXiv:1305.4797](#)].
- [86] A. Paul and D. M. Straub, *Constraints on new physics from radiative B decays*, *JHEP* **04** (2017) 027, [[arXiv:1608.02556](#)].
- [87] B. Grinstein and D. Pirjol, *Exclusive rare $B \rightarrow K^* \ell^+ \ell^-$ decays at low recoil: Controlling the long-distance effects*, *Phys.Rev.* **D70** (2004) 114005, [[hep-ph/0404250](#)].
- [88] C. Bobeth, G. Hiller, and D. van Dyk, *The Benefits of $\bar{B} \rightarrow \bar{K}^* l^+ l^-$ Decays at Low Recoil*, *JHEP* **1007** (2010) 098, [[arXiv:1006.5013](#)].
- [89] M. Beylich, G. Buchalla, and T. Feldmann, *Theory of $B \rightarrow K^{(*)} l^+ l^-$ decays at high q^2 : OPE and quark-hadron duality*, *Eur.Phys.J.* **C71** (2011) 1635, [[arXiv:1101.5118](#)].
- [90] C. Bobeth, G. Hiller, and D. van Dyk, *More Benefits of Semileptonic Rare B Decays at Low Recoil: CP Violation*, *JHEP* **1107** (2011) 067, [[arXiv:1105.0376](#)].
- [91] CMS Collaboration, V. Khachatryan et al., *Angular analysis of the decay $B^0 \rightarrow K^{*0} \mu^+ \mu^-$ from pp collisions at $\sqrt{s} = 8$ TeV*, *Phys. Lett.* **B753** (2016) 424–448, [[arXiv:1507.08126](#)].
- [92] LHCb Collaboration, R. Aaij et al., *Measurements of the S-wave fraction in $B^0 \rightarrow K^+ \pi^- \mu^+ \mu^-$ decays and the $B^0 \rightarrow K^*(892)^0 \mu^+ \mu^-$ differential branching fraction*, *JHEP* **11** (2016) 047, [[arXiv:1606.04731](#)].
- [93] LHCb Collaboration, R. Aaij et al., *Angular analysis of the $B^0 \rightarrow K^{*0} e^+ e^-$ decay in the low- q^2 region*, *JHEP* **04** (2015) 064, [[arXiv:1501.03038](#)].

- [94] J. A. Bailey et al., $B \rightarrow Kl^+l^-$ decay form factors from three-flavor lattice QCD, *Phys. Rev. D* **93** (2016), no. 2 025026, [[arXiv:1509.06235](#)].
- [95] A. Bharucha, D. M. Straub, and R. Zwicky, $B \rightarrow V\ell^+\ell^-$ in the Standard Model from Light-Cone Sum Rules, [arXiv:1503.05534](#).
- [96] **LHCb** Collaboration, R. Aaij et al., Measurement of the ratio of branching fractions $BR(B_0 \rightarrow K^{*0}\gamma)/BR(B_{s0} \rightarrow \phi\gamma)$ and the direct CP asymmetry in $B_0 \rightarrow K^{*0}\gamma$, *Nucl. Phys. B* **867** (2013) 1–18, [[arXiv:1209.0313](#)].
- [97] M. Misiak et al., Updated NNLO QCD predictions for the weak radiative B-meson decays, *Phys. Rev. Lett.* **114** (2015), no. 22 221801, [[arXiv:1503.01789](#)].
- [98] **LHCb** Collaboration, R. Aaij et al., Measurement of the $B_s^0 \rightarrow \mu^+\mu^-$ branching fraction and effective lifetime and search for $B^0 \rightarrow \mu^+\mu^-$ decays, [arXiv:1703.05747](#).
- [99] **CMS** Collaboration, S. Chatrchyan et al., Measurement of the $B_{(s)} \rightarrow \mu^+\mu^-$ branching fraction and search for $B^0 \rightarrow \mu^+\mu^-$ with the CMS Experiment, *Phys. Rev. Lett.* **111** (2013) 101804, [[arXiv:1307.5025](#)].
- [100] C. Bobeth, M. Gorbahn, T. Hermann, M. Misiak, E. Stamou, and M. Steinhauser, $B_{s,d} \rightarrow l^+l^-$ in the Standard Model with Reduced Theoretical Uncertainty, *Phys. Rev. Lett.* **112** (2014) 101801, [[arXiv:1311.0903](#)].
- [101] “Hepfit, a tool to combine indirect and direct constraints on high energy physics.” <http://hepfit.roma1.infn.it/>.
- [102] A. Caldwell, D. Kollar, and K. Kroninger, BAT: The Bayesian Analysis Toolkit, *Comput. Phys. Commun.* **180** (2009) 2197–2209, [[arXiv:0808.2552](#)].
- [103] T. Ando, Predictive bayesian model selection, *American Journal of Mathematical and Management Sciences* **31** (2011), no. 1-2 13–38. <http://dx.doi.org/10.1080/01966324.2011.10737798>.
- [104] A. Gelman, J. B. Carlin, H. S. Stern, and D. B. Rubin, *Bayesian data analysis*. Texts in Statistical Science Series. Chapman & Hall/CRC, Boca Raton, FL, second ed., 2004.
- [105] **Particle Data Group** Collaboration, K. A. Olive et al., *Review of Particle Physics*, *Chin. Phys. C* **38** (2014) 090001.
- [106] **ATLAS, CDF, CMS, D0** Collaboration, First combination of Tevatron and LHC measurements of the top-quark mass, [arXiv:1403.4427](#).
- [107] V. Lubicz. private communication.
- [108] F. Sanfilippo, Quark Masses from Lattice QCD, *PoS LATTICE2014* (2015) 014, [[arXiv:1505.02794](#)].
- [109] S. Aoki et al., Review of lattice results concerning low-energy particle physics, *Eur. Phys. J. C* **74** (2014) 2890, [[arXiv:1310.8555](#)].
- [110] **UTfit** Collaboration, M. Bona et al., The Unitarity Triangle Fit in the Standard Model and Hadronic Parameters from Lattice QCD: A Reappraisal after the Measurements of $\Delta m(s)$ and $BR(B \rightarrow \tau\nu(\tau))$, *JHEP* **10** (2006) 081, [[hep-ph/0606167](#)].
- [111] **UTfit** Collaboration. online update at <http://utfit.org>.
- [112] S. W. Bosch and G. Buchalla, The Radiative decays $B \rightarrow V$ gamma at next-to-leading order in QCD, *Nucl. Phys. B* **621** (2002) 459–478, [[hep-ph/0106081](#)].

- [113] P. Ball and V. M. Braun, *Exclusive semileptonic and rare B meson decays in QCD*, *Phys. Rev.* **D58** (1998) 094016, [[hep-ph/9805422](#)].
- [114] P. Ball and R. Zwicky, *New results on $B \rightarrow \pi, K, \eta$ decay form factors from light-cone sum rules*, *Phys.Rev.* **D71** (2005) 014015, [[hep-ph/0406232](#)].